

Lightning NO_x, a key chemistry-climate interaction: impacts of future climate change and consequences for tropospheric oxidising capacity

Antara Banerjee¹, Alexander T. Archibald^{1,2}, Amanda C. Maycock¹, Paul Telford^{1,2}, N. Luke Abraham^{1,2}, Xin Yang^{1,2,*}, Peter Braesicke^{1,2,**} and John Pyle^{1,2}

¹Department of Chemistry, University of Cambridge, Cambridge, UK

²NCAS-Climate, Department of Chemistry, University of Cambridge, Cambridge, UK

*now at British Antarctic Survey, Cambridge, UK

**now at Karlsruhe Institute of Technology, Institute for Meteorology and Climate Research, Karlsruhe, Germany

Abstract

Lightning is one of the major natural sources of NO_x in the atmosphere. A suite of time-slice experiments using a stratosphere-resolving configuration of the Unified Model (UM), containing the United Kingdom Chemistry and Aerosols sub-model (UKCA), has been performed to investigate the impact of climate change on emissions of NO_x from lightning (LNO_x) and to highlight its critical impacts on photochemical ozone production and the oxidising capacity of the troposphere. Two Representative Concentration Pathway (RCP) scenarios (RCP4.5 and RCP8.5) are explored. LNO_x is simulated to increase in a year-2100 climate by 33% (RCP4.5) and 78% (RCP8.5), primarily as a result of increases in the depth of convection. The total tropospheric chemical odd oxygen production (P(O_x)) increases linearly with increases in total LNO_x and consequently, tropospheric ozone burdens of 29±4 Tg(O₃) (RCP4.5) and 46±4 Tg(O₃) (RCP8.5) are calculated here. By prescribing a uniform surface boundary concentration for methane in these simulations, methane driven feedbacks are essentially neglected. A simple estimate of the contribution of the feedback reduces the increase in ozone burden to 24 and 33 Tg(O₃), respectively. We thus show that, through changes in LNO_x, the effects of climate change counteract the simulated mitigation of the ozone burden, which results from reductions in ozone precursor emissions as part of air quality controls projected in the RCP scenarios. Without the driver of increased LNO_x, our simulations suggest that the net effect of climate change would be to lower free tropospheric ozone.

In addition, we identify large climate-change induced enhancements in the concentration of the hydroxyl radical (OH) in the tropical upper troposphere (UT), particularly over the Maritime Continent, primarily as a consequence of greater LNO_x. The OH enhancement in the tropics increases oxidation of both methane (with feedbacks onto chemistry and climate) and very short-lived substances (VSLS) (with implications for stratospheric ozone depletion). We emphasise that it is important to improve our understanding of LNO_x in order to gain confidence in model projections of composition change under future climate.

1. Introduction

Lightning is one of the primary sources of nitrogen oxides (NO_x=NO+NO₂) in the troposphere and the only natural source remote from the Earth's surface. Emissions of NO_x from lightning (LNO_x) in the mid and upper troposphere (UT), where the NO_x lifetime is longer than at the surface, exert a disproportionately large influence on tropospheric chemistry. Lightning occurs predominantly in regions of strong convection. These regions, and hence LNO_x, are likely to change in a warmer, more moist climate; LNO_x therefore has the potential to be a particularly important factor in chemistry-climate interactions.

LNO_x has several roles relevant to both the composition and the radiative properties of the troposphere. NO_x from lightning induces production of ozone (O₃) in the mid to upper troposphere (e.g. Williams et al., 2005; Schumann and Huntrieser, 2007; Barret et al., 2010), where ozone can exert a particularly strong radiative forcing (Forster and Shine, 1997). The production can be large enough to affect the tropospheric column ozone over or downwind of LNO_x, particularly when other natural sources of NO_x (e.g. biomass burning) are absent (Ryu and Jenkins, 2005).

Concentrations and partitioning of other important trace gases are also affected. For example, the partitioning of the HO_x (HO_x=OH+HO₂) family can be altered by the conversion of HO₂ to OH via the reaction between HO₂ and NO. In addition, formation of HO_x can be induced indirectly, as lightning produced ozone is subsequently photolysed to form O(¹D), which then reacts with water vapour to generate OH. In contrast, HO_x loss ensues when OH and NO₂ react to form nitric acid, which can then be deposited to the surface (Brasseur et al., 2006; Schumann and Huntrieser, 2007). Any changes in HO_x can affect the lifetime of methane, whose loss depends primarily on OH (Holmes et al., 2013; Murray et al., 2013). Since methane is the second most important greenhouse gas in terms of

radiative forcing, this represents an important chemistry-climate feedback resulting from changes in LNO_x.

Changes in climate can also exert a direct influence on LNO_x where, generally, global LNO_x is found to increase in a warmer climate (Grenfell et al., 2003; Zeng and Pyle, 2003; Brasseur et al., 2006; Zeng et al., 2008; Hui and Hong, 2013). However, given the large uncertainty that surrounds present-day LNO_x estimates (generally between 2 and 8 Tg(N) yr⁻¹), its vertical distribution and generation mechanisms (Schumann and Huntrieser, 2007; Wong et al., 2013), future projections are also highly uncertain (Price, 2013). A large part of the uncertainty in future changes arises from deficits in our understanding of the processes that drive modelled changes in convection. Chadwick et al. (2013) analysed tropical convective mass fluxes in the models contributing to the recent Coupled Model Intercomparison Project phase 5 (CMIP5) and found both a climatological weakening and a deepening of convection to be robust responses to a warmer climate. The depth of convection is likely to increase due, at least in part, to an uplifting of the tropopause with climate change. However, the mechanisms behind the changes in convection are complicated by several potential contributing factors and are still under debate. These factors might include: increasing sea-surface temperatures (SSTs) (Ma et al., 2012; Ma et al., 2013; Chadwick et al., 2013), spatial changes in SST patterns (Xie et al., 2010), increases in the static stability of the lower atmosphere (as the upper troposphere warms more than the lower troposphere) (Chadwick et al., 2012) and increases in the depth of convection itself (Chou et al., 2009; Chou and Chen, 2010). With these uncertainties in mind, it is nonetheless important to explore the possible feedback processes involving LNO_x in a future climate.

To do this, we use a stratosphere-resolving configuration of the Unified Model (UM) containing the United Kingdom Chemistry and Aerosols (UKCA) sub-model with both stratospheric and tropospheric chemistry, to perform a series of sensitivity experiments perturbing perpetual year-2000 conditions to year-2100. In these experiments, we explore climate change using two Representative Concentration Pathway (RCP) scenarios: RCP4.5 and RCP8.5 (IPCC, 2013); we also change the concentrations of ozone-depleting substances (ODS) and tropospheric ozone precursor emissions. The focus in this study lies in examining changes in LNO_x and subsequent impacts on tropospheric composition. We do not attempt to provide a detailed description of all the changes associated with the applied perturbations; that will form the basis of a future publication.

The following sections are organised as follows. Section 2 describes the experimental set-up and the method in which LNO_x is calculated in UM-UKCA. Section 3 then discusses

the impacts of future climate change on LNO_x. The associated changes in tropospheric ozone and oxidising capacity are highlighted. Section 4 concludes with a summary of the results.

2. Model description

2.1 Experimental set-up

We use UM-UKCA in its atmosphere-only set-up at N48L60 resolution ($3.75^\circ \times 2.5^\circ$ with 60 hybrid-height levels extending up to 84km). The dynamical core is described by Hewitt et al. (2011). The model is forced by prescribed sea surface temperatures (SSTs) and sea ice. A uniform concentration for CO₂ is assumed while uniform surface boundary conditions are prescribed for the remaining greenhouse gases (GHGs) and ozone-depleting substances (ODS) (N₂O, methane and halogen-containing species). These can be varied independently within the radiation and chemistry schemes. There are surface emissions of 9 species (NO, CO, HCHO, C₂H₆, C₃H₈, CH₃COCH₃, CH₃CHO, C₅H₈ and biogenic CH₃OH) and multi-level emissions for NO_x emitted from aircraft.

The chemistry scheme used is a combination of the well-established tropospheric (O'Connor et al., 2014) and stratospheric (Morgenstern et al., 2009) schemes. It includes the O_x, HO_x and NO_x chemical cycles and the oxidation of CO, ethane, propane, and isoprene (Archibald et al., 2011), in addition to chlorine and bromine chemistry, including heterogeneous processes on polar stratospheric clouds (PSCs) and liquid sulfate aerosols. Photolysis is calculated interactively by the Fast-JX scheme (Telford et al., 2013) and ozone is coupled interactively between chemistry and radiation.

We perform a series of time-slice integrations with fixed boundary conditions. For each, we allow the model to spin up for 10 years and integrate for a further 10 years. Through a total of 10 different simulations, we evaluate the response of the model to three types of perturbations and their combinations. The full set of simulations is summarised in Table 1. The Base run is defined by year-2000 boundary conditions.

The separate perturbations are described as follows:

i) Climate change (CC) - The climate is changed by varying concentrations of GHGs (CO₂, methane, N₂O, CFCs and HCFCs) in the radiation scheme, and prescribed SST/sea ice fields. The changes in GHGs are not imposed in the chemistry scheme. We adopt three different realisations for climate: a) year 2000, b) year 2100, RCP4.5, and c) year 2100, RCP8.5. For year 2000, GHGs are fixed at historical concentrations for this year according to the RCP dataset (van Vuuren et al., 2011); the SST/sea ice fields are obtained from the observational

HadISST dataset (Rayner et al., 2003) and are averages over the years 1998-2002. For year 2100, GHG concentrations are specified according to the concentrations in the RCP4.5 or RCP8.5 scenarios; the SST/sea ice fields are obtained from simulations using the HadGEM2-CC coupled atmosphere-ocean model for these respective scenarios (Martin et al., 2011) and are averages over the years 2081-2100 (RCP4.5) and 2091-2100 (RCP8.5).

ii) Ozone-depleting substances (ODS) - Changes in ODS are imposed only within the chemistry scheme; for radiatively active ODS (e.g. CFC-11 and CFC-12), these changes are decoupled from the radiation scheme. We only consider future changes in halogen-containing species, while N_2O and methane, which are source gases for ODS, are left unchanged. For year 2000, we apply historical surface concentrations obtained from the RCP dataset; for year 2100, we apply the concentrations projected by the RCP4.5 scenario.

iii) Ozone precursor emissions (O_3pre) - We consider a future reduction in the anthropogenic components of emissions relative to year-2000 values as according to the RCP4.5 scenario. Emissions from natural sources, including isoprene emissions, remain unchanged. Methane is also not changed in the chemical scheme.

We aim to isolate the impact of LNO_x from other effects of climate change by performing two further simulations in which we fix LNO_x but allow climate (and its influence on convection) to vary between them. These are the Base(f LNO_x) and $\Delta\text{CC8.5}(\text{fLNO}_x)$ simulations which are run under year-2000 and year-2100 RCP8.5 climate, respectively. In these, both the amount and distribution of LNO_x are fixed to that of the Base run. To do this, we switch off the interactive calculation of LNO_x (see Sect. 2.2) and instead, impose a monthly mean climatology of these emissions obtained from the Base run, which is linearly interpolated to 5-day averages. The Base(f LNO_x) and Base runs should be identical; indeed, there are negligible differences in temperature, tropospheric ozone and OH between these runs, providing validation for the method of imposing an LNO_x climatology. It is therefore also valid to present results of $\Delta\text{CC8.5}(\text{fLNO}_x)$ as differences from Base (as with all other perturbations in this study), with the confidence that there are no differences generated from the contrasting experimental set-ups. Base(f LNO_x) will henceforth not be discussed and $\Delta\text{CC8.5}(\text{fLNO}_x)$ will be referred to as the “fixed- LNO_x ” run.

2.2 Lightning NO_x parameterisation

LNO_x is calculated every hour in UM-UKCA following the method applied in the p-TOMCAT model. Details of the methodology are provided in Barret et al. (2010) and

references therein but a brief description is provided here. Lightning flash frequencies are parameterised according to the Price and Rind (1992, 1994a) scheme (henceforth abbreviated as PR92):

$$F_c = 3.44 \times 10^{-5} H^{4.9} \quad (1)$$

$$F_m = 6.40 \times 10^{-4} H^{1.73} \quad (2)$$

where F_c and F_m are continental and marine lightning frequencies (flashes $\text{minute}^{-1} 25\text{km}^{-2}$), respectively, and H is the cloud-top height (kilometres), which is determined from the model convection scheme. The PR92 method for calculating the proportion of cloud-to-ground (CG) and intra-cloud (IC) flashes is incorporated, but here, the energy per flash is constant regardless of the type of flash. 10^{26} molecules of NO are produced per flash and the flash frequencies are scaled to match observations of the present-day (Barret et al., 2010), resulting in 6 Tg(N) yr^{-1} of total, global LNO_x for the year 2000. The scaling factor is unchanged between runs, such that LNO_x will vary only with changes in convective cloud-top height through changes in convection. The molecules of NO_x produced in each column are then distributed evenly in log-pressure coordinates from 500 hPa to the cloud-top and the ground to 500 hPa for IC and CG flashes, respectively.

Implementation of the PR92 scheme varies in its details from model to model, generally with an aim to generate lightning flash frequencies and distribution for the present-day atmosphere (as within the development of UM-UKCA) or for a particular choice of total, global LNO_x . In a model study, Labrador et al. (2005) have demonstrated that, in addition to the overall magnitude of LNO_x , concentrations of tropospheric trace constituents are also particularly sensitive to the vertical distribution of LNO_x . However, they were unable to select a best fitting distribution due to the low number of observational campaigns and the large scatter in existing data. Compared to other vertical LNO_x distributions, such as those suggested by Pickering et al. (1998) and Ott et al. (2010), UKCA distributes LNO_x more evenly by mass in the vertical. As a result, UKCA would simulate lower ozone and OH in the mid and upper troposphere for a given magnitude of total LNO_x , relative to these distributions. In the lower troposphere and the boundary layer, where NO_x lifetimes are short, trace gas concentrations are far less sensitive to LNO_x (Labrador et al., 2005).

Convection itself is also parameterised at the horizontal resolution used in this model and in most current chemistry-climate and chemical transport models (CCMs, CTMs). Russo et al. (2011) showed that although a high vertical model resolution is needed to match the

vertical distribution of clouds to observations, a low horizontal resolution is sufficient to capture the geographical distribution.

As in many sensitivity studies, we bear these caveats in mind and use our parameterisations as reference schemes relative to which we study changes. Our goal is thus to understand the mechanisms by which climate change could drive changes in chemistry, with a focus on the role of LNO_x , rather than attempt to predict the future state of the atmosphere.

3. Results

We primarily address changes related to LNO_x between the runs outlined in Sect. 2.1. We will first discuss changes in the LNO_x amount and distribution with climate change in Sect. 3.1. Then, in Sect. 3.2, we will show the resulting impacts on the tropospheric, global odd oxygen budget. In Sect. 3.3, we will address consequences for the OH radical, which principally determines the oxidising capacity of the troposphere, and finally, we will discuss the associated impacts on methane and other trace gases in Sect. 3.4.

3.1 Changes in LNO_x

The fifth column in Table 1 shows that experiments with a warmer climate simulate greater LNO_x . Relative to the year-2000 climate, there are substantial increases in LNO_x of 2 Tg(N) yr^{-1} (33%) and 4.7 Tg(N) yr^{-1} (78%) between runs for which only the climate changes, according to the RCP4.5 and RCP8.5 scenarios, respectively. This corresponds to a sensitivity of 0.96 Tg(N) K^{-1} or 16% K^{-1} although the relationship between LNO_x and global mean surface temperature is not quite linear (not shown). This sensitivity is stronger than that reported by some previous model studies: 9% K^{-1} (Brasseur et al., 2006), 12% K^{-1} (Grenfell et al., 2003), 5-6% K^{-1} (Price and Rind, 1994b). This could reflect differences in the specific tuning of the PR92 parameterisation (used in all of these cited studies), in convection schemes and/or in the model resolutions.

With regard to its geographical distribution, LNO_x occurs predominantly over the tropics in regions which show high convective activity: South America, Central Africa and the West Pacific/Maritime Continent. Figure 1 shows changes in the tropically averaged (20°S - 20°N), annual mean distribution of LNO_x between Base and the runs which change climate only (Fig. 1a: $\Delta\text{CC4.5}$ and Fig. 1b: $\Delta\text{CC8.5}$). Increases in LNO_x occur primarily over

the Maritime Continent for $\Delta\text{CC4.5}$. $\Delta\text{CC8.5}$ displays, in addition, large increases over Central Africa and South America, highlighting the potential importance of all three regions with respect to future changes in LNO_x . In contrast to the study of Hui and Hong (2013), in which the Maritime Continent displays the weakest increases in LNO_x by 2050 (except in boreal winter when they are comparable to the increases over South America), this region is associated with the largest changes in LNO_x in UM-UKCA for all months of the year and both RCP scenarios. These opposing results might be attributable to a difference in model resolutions. Compared to UM-UKCA, the coarser resolution ($4^\circ \times 5^\circ$) GEOS-Chem model used by Hui and Hong (2013) is less able to resolve the islands and peninsulas of the Maritime Continent, which may result in systematic biases in LNO_x over this region.

Changes in LNO_x can result from changes in both the intensity (depth) of individual convective events and the overall frequency of convection. Distributions of convective cloud-top height (CTH) (not shown) indicate a shift towards greater CTH under future climate change. For example, in $\Delta\text{CC8.5}$, mean CTH increases by 23.6% (Maritime Continent), 9.3% (Africa) and 4.6% (South America) relative to Base, where the regions are defined as in Russo et al. (2011). These increases in the depth of convection are consistent with rising tropopause heights (Fig. 1). Using the number of CTH occurrences as a crude measure of the overall frequency of convective events, we find increases of 12.4% and 3.6% over the Maritime Continent and Africa, respectively, but a decrease of 5.2% over South America in $\Delta\text{CC8.5}$. Since the PR92 parameterisation for LNO_x is highly sensitive to the magnitude of CTH, it is the increases in the depth of convection, scaling with the climate forcing, which primarily lead to increases in LNO_x in our simulations. The effect of the parameterisation is highlighted over South America in $\Delta\text{CC8.5}$, where, although convection occurs less often on average, LNO_x still increases due to an increase in the depth of convection. The largest increases in LNO_x occur over the Maritime Continent because this region is associated with the largest increases in both the frequency and depth of convection.

3.2 Changes in ozone

As a global measure of changes in ozone, we have analysed the tropospheric budget of odd oxygen (O_x), of which chemical production ($\text{P}(\text{O}_x)$) represents one term. Since LNO_x is one driver of $\text{P}(\text{O}_x)$, we first study the correlation between $\text{P}(\text{O}_x)$ and LNO_x , shown in Fig. 2a. For each set of experiments (i.e. climate change; climate change plus changes in ODS; and climate change plus changes in tropospheric ozone precursors), a highly linear fit between the

changes in $P(O_x)$ and LNO_x is found. Within this ensemble of simulations, we find that increases in LNO_x with climate change are concurrent with increases in $P(O_x)$ of 413 ± 28 $Tg(O_3) \text{ yr}^{-1}$ and 977 ± 33 $Tg(O_3) \text{ yr}^{-1}$ for the RCP4.5 and RCP8.5 scenarios, respectively, where the reported ranges represent the interannual variability as one standard deviation.

Figure 2a allows for an assessment of the importance of climate change versus non-climate change related impacts on $P(O_x)$. Reductions in $P(O_x)$ of approximately $100 \text{ Tg}(O_3) \text{ yr}^{-1}$ due to removal of ODS (green line, Fig. 2a) are small in magnitude relative to climate-change driven increases. Runs containing reduced emissions of anthropogenic ozone precursors (red line, Fig. 2a) show approximately $800 \text{ Tg}(O_3) \text{ yr}^{-1}$ lower $P(O_x)$ than corresponding runs without (blue line). However, for the RCP8.5 scenario, this reduction is more than cancelled by the effect of climate change on LNO_x , such that $P(O_x)$ in $\Delta(CC8.5+O3pre)$ is greater than in Base.

$P(O_x)$ represents one of four contributing terms to the global burden of ozone in the troposphere, the others being chemical loss ($L(O_x)$), deposition and stratosphere-troposphere exchange (STE). A future publication will discuss the effect of the applied perturbations on these terms in detail. Here, we simply note that LNO_x driven increases in $P(O_x)$ induced by climate change represent a significant contribution to the increases in ozone burden of 29 ± 4 $Tg(O_3)$ for RCP4.5 and 46 ± 4 $Tg(O_3)$ for RCP8.5, as shown in Table 1 and Fig. 2b. In contrast to $P(O_x)$, the changes in ozone burden and LNO_x are non-linearly related, since several factors, and not just LNO_x , contribute significantly to changes in the burden in a warmer climate. From Fig. 2b, it is also evident that the decrease in burden of 34 ± 4 $Tg(O_3)$ due to $\Delta O3pre$ is just outweighed by the increase in $\Delta(CC8.5+O3pre)$, although by using a fixed methane surface concentration in these simulations, the additional feedbacks on ozone and OH are not included (see Sect. 3.4). Nevertheless, it appears that reductions in the ozone burden due to emission policies could be counteracted by future changes in climate.

To confirm that LNO_x is the dominant factor leading to increases in $P(O_x)$ and the ozone burden, we examine the $\Delta CC8.5(fLNO_x)$ simulation, which includes RCP8.5 climate forcings but with LNO_x taken from the Base run rather than calculated online. Table 2 shows numerical changes in the tropospheric O_x budget terms for the $\Delta CC8.5$ and $\Delta CC8.5(fLNO_x)$ runs relative to Base. With fixed LNO_x , $P(O_x)$ increases by only 7.0% as compared to 20.1% when LNO_x is allowed to vary with climate change. There is strong buffering in the response of the burden by the loss terms: fixing LNO_x also leads to smaller magnitude changes in loss through $L(O_x)$ and deposition. Overall however, there is a greater decrease in net chemical production ($P(O_x)$ minus $L(O_x)$) from Base for $\Delta CC8.5(fLNO_x)$ than for $\Delta CC8.5$.

Table 2 shows that we also find a smaller increase in STE when fixing LNO_x. Comparing Fig. 3a and b gives one possible explanation: without increases in LNO_x and consequently upper tropospheric ozone, the amount of ozone in the lower stratosphere is reduced (following entry into the tropical lower stratosphere and quasi-horizontal mixing). In the mid-latitudes, this would reduce the STE of ozone back into the troposphere. Thus, in our model, we estimate that the increase in LNO_x with climate change at RCP8.5 contributes 6.4% to the increase in STE.

Importantly, the balance between the budget terms means that, without inclusion of changes in LNO_x, there results a slight decrease (-5.8%) rather than an increase (13.2%) in the ozone burden with climate change at RCP8.5. In fact, the decrease in ozone is seen throughout the troposphere in the zonal and annual mean (Fig. 3b), primarily due to increased humidity in a warmer climate (e.g. Thompson et al., 1989). Hence, these results suggest that climate change would enhance possible future mitigation of free tropospheric ozone if LNO_x were not to increase in a warmer climate.

3.3 Changes in OH

The impacts of LNO_x extend to other chemical species. Figure 4 illustrates changes in the tropically averaged (20°S-20°N), annual mean distribution of OH for ΔCC4.5, ΔCC8.5 and ΔCC8.5(fLNO_x) as absolute (a-c) and relative differences (d-f) from Base. Regions of OH enhancement in Fig. 4 correspond to regions of increased LNO_x in Fig. 1. The Maritime Continent, which experiences the greatest increases in LNO_x in these simulations, also displays the strongest enhancements in OH. Figure 4 shows that these changes are large, with a peak of over 0.2 ppt (100%) for ΔCC4.5 and 0.3 ppt (160%) for ΔCC8.5. An analysis of species concentrations and reaction fluxes indicates that these changes in OH are due to a combination of:

- i) direct chemical conversion of HO₂ to OH via NO emitted from lightning;
- ii) deeper convection transporting water vapour into these regions of the UT and hence inducing OH production through O(¹D)+H₂O;
- iii) feedbacks through other chemical species e.g. ozone produced following process i) can photolyse to produce O(¹D) and induce OH production, once again, through O(¹D)+H₂O.

We examined process ii) in isolation by switching LNO_x changes off in the model in the ΔCC8.5(fLNO_x) simulation. So, when LNO_x increases are ignored (Fig. 4c and f), we only

find an increase in OH over the Maritime Continent, amounting to about 20%. OH decreases elsewhere, indicating that an increase in water vapour transport into the tropical UT is not the dominant process controlling OH increases with climate change throughout that region. In contrast, our analysis shows that LNO_x increases the flux through HO₂+NO (process i) and, as a result, also through O(¹D)+H₂O (process iii) throughout the tropical UT.

3.4 Consequences for methane and other trace gases

Since OH is the primary tropospheric oxidant, substantial enhancements in its abundance, such as those shown in Sect. 3.3, can have ramifications for a range of other chemical species. For example, oxidation by OH is the main loss process for atmospheric methane. Hence, there are potentially global consequences through perturbation of the methane lifetime. A measure of this effect can again be deduced from the ΔCC8.5(fLNO_x) run. Relative to Base, a reduction of 1.79 years in the methane lifetime against loss by OH ($\tau_{\text{CH}_4+\text{OH}}$) is calculated for ΔCC8.5; in contrast, a smaller reduction of 1.04 years is found for ΔCC8.5(fLNO_x). Inclusion of changes in LNO_x thus contributes 0.75 years to the reduction in $\tau_{\text{CH}_4+\text{OH}}$ due to climate change.

Changes in $\tau_{\text{CH}_4+\text{OH}}$ will have implications for both chemistry and climate through methane's role as a tropospheric ozone precursor, an OH sink and a greenhouse gas. However, by fixing a uniform lower boundary condition for methane, such feedbacks are essentially neglected within these experiments. If methane concentrations were allowed to respond to decreases in its lifetime with climate change, lower methane concentrations would be simulated at equilibrium in a future climate, with a lower increase in ozone burden and an enhanced increase in OH. The strength of the response is determined by the model dependent methane feedback factor, f (Fuglestad et al., 1999). Using a further integration in which methane is increased by 20% in the chemistry scheme only (not otherwise discussed here), we derive a value of 1.52 for f in our model, which lies on the upper end of the large literature range (1.19-1.53) (Prather, 2001; Voulgarakis et al., 2013; Stevenson et al., 2013). From this, we obtain an estimate of equilibrium methane concentrations, following the methodology detailed in Stevenson et al. (2013), and equilibrium ozone burdens, following Wild et al. (2012). We find that accounting for methane adjustments lowers the ozone burden in future climate simulations by, on average, 5 Tg(O₃) (RCP4.5) and 13 Tg(O₃) (RCP8.5). The corresponding increases in ozone burden relative to Base are 24 Tg(O₃) (RCP4.5) and 33 Tg(O₃) (RCP8.5), which still represent substantial increases with future climate change and

greater LNO_x. The adjusted increase in burden in $\Delta(\text{CC8.5}+\text{O3pre})$ (33 Tg(O₃)) is now more comparable to the adjusted decrease in ΔO3pre (32 Tg(O₃)).

OH is also important in determining the lifetime of very short-lived substances (VSLS). There is currently considerable interest in the role of VSLS in stratospheric ozone depletion following rapid convective transport into the upper troposphere-lower stratosphere (UTLS) region. Increased oxidation of VSLS by OH in the UT in a future climate could serve to counteract increased stratospheric VSLS loading following enhanced convective lofting into the tropical tropopause layer (TTL) and subsequent transport into the lower stratosphere. The effect could be particularly important over the Maritime Continent, since it is a region characterised by both high deep convective activity and coastal emissions of VSLS (Hosking et al., 2010). These feedbacks add weight to the importance of future changes in LNO_x.

4. Summary

We have assessed the impacts of climate change on emissions of NO_x from lightning (LNO_x) and the consequences for tropospheric chemistry using UM-UKCA. Using the Price and Rind (1992, 1994a) parameterisation for calculation of LNO_x, our year-2000 integrations generate 6 Tg(N) yr⁻¹ of total, global LNO_x, which lies within the range of values simulated in the literature (e.g. Schumann and Huntrieser, 2007) and within 1 σ of the ACCMIP multi-model mean (Young et al., 2013). We simulate greater LNO_x at the year 2100 under two scenarios for future climate change: RCP4.5 and RCP8.5, with LNO_x increases of 2 Tg(N) yr⁻¹ (33%) and 4.7 Tg(N) yr⁻¹ (78%), respectively, primarily in response to increases in the depth of convection. These correspond to a greater sensitivity of LNO_x to climate than found in some other studies and the total LNO_x simulated for RCP8.5 is above 1 σ of the ACCMIP models. The sensitivity will depend upon the treatment of convection and LNO_x in the different models; these remain an area of considerable uncertainty. Note that we have not explored other LNO_x parameterisations and some studies using alternate approaches, such as those based on convective mass fluxes, have found different sensitivities for lightning changes under a warmer climate (e.g. Grewe et al., 2009). However, the PR92 method employed here is commonly adopted in state-of-the-art chemistry-climate models, such as most of the ACCMIP models (Lamarque et al., 2013).

For the simulations which change climate only between the years 2000 and 2100, according to RCP4.5 ($\Delta\text{CC4.5}$) and RCP8.5 ($\Delta\text{CC8.5}$), we also analysed changes in the distribution of LNO_x within the tropics. Increases in LNO_x are found to occur predominantly

over the Maritime Continent for $\Delta\text{CC4.5}$ but also over Central Africa and South America for $\Delta\text{CC8.5}$. The Maritime Continent is associated with the largest increases in both the overall frequency and depth of convection, which explains the largest increases in LNO_x found over this region.

A positive and linear relationship is simulated between the changes in LNO_x and global, tropospheric chemical O_x production ($\text{P}(\text{O}_x)$), which increases by $413 \pm 28 \text{ Tg}(\text{O}_3) \text{ yr}^{-1}$ and $977 \pm 33 \text{ Tg}(\text{O}_3) \text{ yr}^{-1}$ for climate change under the RCP4.5 and RCP8.5 scenarios, respectively. The tropospheric ozone burden increases correspondingly by $29 \pm 4 \text{ Tg}(\text{O}_3)$ (RCP4.5) and $46 \pm 4 \text{ Tg}(\text{O}_3)$ (RCP8.5). We confirm through a fixed- LNO_x run that LNO_x plays the major role in these correlations, contributing more than 50% to the increase in $\text{P}(\text{O}_x)$ at RCP8.5. We also show that the effects of climate change, at least for the RCP8.5 scenario, would decrease the ozone burden if this effect on $\text{P}(\text{O}_x)$ through LNO_x were not present.

To examine the sensitivity of the effects of climate change to the background state of the atmosphere, three sets of experiments were conducted which combined the separate climate forcings with different chemical drivers: i) year-2000 chemical boundary conditions, ii) lower concentrations of stratospheric ozone-depleting substances, and iii) lower emissions of tropospheric ozone precursors. The linear relationship between the increases in LNO_x and $\text{P}(\text{O}_x)$ and the corresponding increases in tropospheric ozone burden under climate change are found to be quantitatively robust under the different chemical background states. Hence, although we find that regulations aimed at air quality improvement decrease the future tropospheric burden of ozone in the ΔO3pre simulation, we suggest that climate change and increased LNO_x could counteract this change.

Changes in LNO_x impact on the OH radical. Our $\Delta\text{CC4.5}$ and $\Delta\text{CC8.5}$ simulations show positive anomalies in upper tropospheric OH over Central Africa, South America and the Maritime Continent. The effect is greatest over the Maritime Continent in both these simulations and is particularly large in $\Delta\text{CC8.5}$, in which an increase of over 160% is found in this region. The response is not reproduced by the fixed- LNO_x run, leading us to conclude that LNO_x drives these changes in OH, although we also find a smaller contribution from deeper convection over the Maritime Continent. An analysis of reaction fluxes indicates that the dominant reaction pathways for increased OH production through LNO_x in these regions are $\text{HO}_2 + \text{NO}$ (directly, following production of NO_x) and $\text{O}(^1\text{D}) + \text{H}_2\text{O}$ (indirectly, through photochemical ozone and hence $\text{O}(^1\text{D})$ production).

Changes in OH could have further important consequences. For methane, we quantify the LNO_x -OH driven impact on its lifetime against loss by OH ($\tau_{\text{CH}_4 + \text{OH}}$) using the fixed-

LNO_x run. LNO_x contributes 0.75 years to the decrease in $\tau_{\text{CH}_4+\text{OH}}$ projected under climate change at RCP8.5. The resulting changes in methane concentration and subsequent feedbacks are not simulated by these experiments. Since methane is both a tropospheric ozone precursor and an OH sink, we expect that a shorter $\tau_{\text{CH}_4+\text{OH}}$ would feedback negatively into LNO_x driven increases in ozone but positively into increases in OH. For ozone, we have estimated that accounting for adjustments in methane concentration in a changing climate would lead to increases in the ozone burden of 24 Tg(O₃) (RCP4.5) and 33 Tg(O₃) (RCP8.5). Although, as expected, these are smaller than the simulated changes reported above (of 29 and 46 Tg(O₃), respectively), they still represent substantial increases through future climate change. Since methane is a greenhouse gas, we would also expect a negative feedback into climate change through its radiative forcing effect.

In addition, very short-lived substances (VSLS), which have a strong source region in the Maritime Continent and are convectively lifted into the UT, could undergo enhanced oxidation by OH if the levels of the latter were to increase over this region. Some studies (e.g. Dessens et al., 2009; Hossaini et al., 2012) project an increase in concentrations of VSLS or their oxidised products in the UTLS, which deplete ozone if they remain in the stratosphere. LNO_x-derived OH could partially offset this effect in a future climate.

We have demonstrated that NO_x production from lightning, following tropical convection, is a key process through which climate can influence the chemistry of the troposphere. Hence, given its importance, we believe it is crucial to strengthen our confidence in model representations of both convection and LNO_x. Our results are dependent on the LNO_x and convective parameterisations utilised. In particular, the vertical profile of LNO_x affects the simulated changes in ozone and OH, particularly in the UT (Labrador et al., 2005). If we were to employ the vertical distributions of Pickering et al. (1998) or Ott et al. (2010), which weight LNO_x more greatly to the UT than is done in UKCA, we postulate that even larger changes in ozone, OH and subsequent feedbacks would occur for a given change in total LNO_x.

Acknowledgements

We thank the ERC for support under the ACCI project, Project No. 267760. ATA was supported by a fellowship from the Hershel Smith Foundation. ACM was supported by a postdoctoral fellowship from the AXA Research Fund.

461

462 **References**

463 Archibald, A. T., Levine, J. G., Abraham, N. L., Cooke, M. C., Edwards, P. M., Heard, D. E.,
464 Jenkin, M. E., Karunaharan, A., Pike, R. C., Monks, P. S., Shallcross, D. E., Telford, P. J.,
465 Whalley, L. K. and Pyle, J. A.: Impacts of HOx regeneration and recycling in the oxidation of
466 isoprene: consequences for the composition of past, present and future atmospheres,
467 *Geophys. Res. Lett.*, 38, L05804, doi:10.1029/2010GL046520, 2011.

468 Barret, B., Williams, J. E., Bouarar, I., Yang, X., Josse, B., Law, K., Pham, M., Le
469 Flochmoën, E., Liousse, C., Peuch, V. H., Carver, G. D., Pyle, J. A., Sauvage, B., van
470 Velthoven, P., Schlager, H., Mari, C. and Cammas, J.-P.: Impact of West African Monsoon
471 convective transport and lightning NOx production upon the upper tropospheric composition:
472 a multi-model study, *Atmos. Chem. Phys.*, 10, 5719-5738, doi:10.5194/acp-10-5719-2010,
473 2010.

474 Brasseur, G. P., Schultz, M. G., Granier, C., Saunois, M., Diehl, T., Botzet, M. and Roeckner,
475 E.: Impact of climate change on the future chemical composition of the global troposphere, *J.*
476 *Clim.*, 19, 3932-3951, doi:10.1175/JCLI3832.1, 2006.

477 Chadwick, R., Wu, P., Good, P. and Andrews, T.: Asymmetries in tropical rainfall and
478 circulation patterns in idealised CO₂ removal experiments, *Clim. Dyn.*, 40, 295-316,
479 doi:10.1007/s00382-012-1287-2, 2012.

480 Chadwick, R., Boutle, I. and Martin, G.: Spatial patterns of precipitation change in CMIP5:
481 why the rich do not get richer in the tropics, *J. Clim.*, 26, 3803-3822, doi:10.1175/JCLI-D-12-
482 00543.1, 2013.

483 Chou, C. and Chen, C.-A.: Depth of convection and the weakening of tropical circulation in
484 global warming, *J. Clim.*, 23, 3019-3030, doi:10.1175/2010JCLI3383.1, 2010.

485 Chou, C., Neelin, J. D., Chen, C.-A. and Tu, J.-Y.: Evaluating the “rich-get-richer”
486 mechanism in tropical precipitation change under global warming, *J. Clim.*, 22, 1982-2005,
487 doi:10.1175/2008JCLI2471.1, 2009.

488 Dessens, O., Zeng, G., Warwick, N. and Pyle, J.: Short-lived bromine compounds in the
489 lower stratosphere; impact of climate change on ozone, *Atmos. Sci. Lett.*, 10, 201-206,
490 doi:10.1002/asl.236, 2009.

491 Forster, P. M. d. F., and Shine, K. P.: Radiative forcing and temperature trends from
 492 stratospheric ozone changes, *J. Geophys. Res.*, 102, 10841-10855, doi:10.1029/96JD03510,
 493 1997.

494 Fuglestvedt, J. S., Berntsen, T. K., Isaksen, I. S. A., Mao, H., Liang, X.-Z. and Wang, W.-C.:
 495 Climatic forcing of nitrogen oxides through changes in tropospheric ozone and methane;
 496 global 3D model studies, *Atmos. Environ.*, 33, 961-977, 1999.

497 Grenfell, J. L., Shindell, D. T. and Grewe, V.: Sensitivity studies of oxidative changes in the
 498 troposphere in 2100 using the GISS GCM, *Atmos. Chem. Phys.*, 3, 1267-1283,
 499 doi:10.5194/acpd-3-1805-2003, 2003.

500 Grewe, V., Impact of Lightning on Air Chemistry and Climate, in: *Lightning: Principles,*
 501 *Instruments and Applications, Review of Modern Lightning Research*, edited by: Betz, H. D.,
 502 Schumann, U., Laroche, P., Springer Science+Business Media B. V., 524-551,
 503 doi:10.1007/978-1-4020-9079-0_25, 2009.

504 Hewitt, H. T., Copsey, D., Culverwell, I. D., Harris, C. M., Hill, R. S. R., Keen, A. B.,
 505 McLaren, A. J. and Hunke, E. C.: Design and implementation of the infrastructure of
 506 HadGEM3: the next-generation Met Office climate modelling system, *Geosci. Model. Dev.*,
 507 4, 223-253, doi:10.5194/gmd-4-223-2011, 2011.

508 Holmes, C. D., Prather, M. J., Søvde, O. A. and Myhre, G.: Future methane, hydroxyl, and
 509 their uncertainties: key climate and emission parameters for future predictions, *Atmos. Chem.*
 510 *Phys.*, 13, 285-302, doi:10.5194/acp-13-285-2013, 2013.

511 Hosking, J. S., Russo, M. R., Braesicke, P. and Pyle, J. A.: Modelling deep convection and its
 512 impacts on the tropical tropopause layer, *Atmos. Chem. Phys.*, 10, 11175-11188,
 513 doi:10.5194/acp-10-11175-2010, 2010.

514 Hossaini, R., Chipperfield, M. P., Dhomse, S., Ordóñez, C., Saiz-Lopez, A., Abraham, N. L.,
 515 Archibald, A., Braesicke, P., Telford, P., Warwick, N., Yang, X. and Pyle, J.: Modelling
 516 future changes to the stratospheric source gas injection of biogenic bromocarbons, *Geophys.*
 517 *Res. Lett.*, 39, L20813, doi:10.1029/2012GL053401, 2012.

518 Hui, J. and Hong, L.: Projected changes in NO_x Emissions from lightning as a result of 2000–
 519 2050 climate change, *Atmos. Oceanic Sci. Lett.*, 6, 284-289, doi: 10.3878/j.issn.1674-
 520 2834.13.0042, 2013.

521 IPCC: Climate Change 2013: The Physical Science Basis. Contribution of Working Group I
 522 to the Fifth Assessment Report of the Intergovernmental Panel on Climate Change, edited by:
 523 Stocker, T. F., Qin, D., Plattner, G.-K., Tignor, M., Allen, S. K., Boschung, J., Nauels, A.,
 524 Xia, Y., Bex, V., and Midgley, P. M., Cambridge University Press, Cambridge, United
 525 Kingdom and New York, NY, USA, 2013.

526 Labrador, L. J., Kuhlmann, R. V. and Lawrence, M. G.: The effects of lightning-produced
 527 NO_x and its vertical distribution on atmospheric chemistry: sensitivity simulations with
 528 MATCH-MPIC, *Atmos. Chem. Phys.*, 5, 1815-1834, doi:10.5194/acp-5-1815-2005, 2005.

529 Lamarque, J.-F., Shindell, D. T., Josse, B., Young, P. J., Cionni, I., Eyring, V., Bergmann, D.,
 530 Cameron-Smith, P., Collins, W. J., Doherty, R., Dalsoren, S., Faluvegi, G., Folberth, G.,
 531 Ghan, S. J., Horowitz, L. W., Lee, Y. H., MacKenzie, I. A., Nagashima, T., Naik, V.,
 532 Plummer, D., Righi, M., Rumbold, S. T., Schulz, M., Skeie, R. B., Stevenson, D. S., Strode,
 533 S., Sudo, K., Szopa, S., Voulgarakis, A. and Zeng, G.: The Atmospheric Chemistry and
 534 Climate Model Intercomparison Project (ACCMIP): overview and description of models,
 535 simulations and climate diagnostics, *Geosci. Model Dev.*, 6, 179-206, doi:10.5194/gmd-6-
 536 179-2013, 2013.

537 Ma, J. and Xie, S.-P.: Regional patterns of sea surface temperature change: a source of
 538 uncertainty in future projections of precipitation and atmospheric circulation, *J. Clim.*, 26,
 539 2482-2501, doi:10.1175/JCLI-D-12-00283.1, 2013.

540 Ma, J., Xie, S.-P. and Kosaka, Y.: Mechanisms for tropical tropospheric circulation change in
 541 response to global warming, *J. Clim.*, 25, 2979-2994, doi:10.1175/JCLI-D-11-00048.1, 2012.

542 Martin, G. M., Bellouin, N., Collins, W. J., Culverwell, I. D., Halloran, P. R., Hardiman, S.
 543 C., Hinton, T. J., Jones, C. D., McDonald, R. E., McLaren, A. J., O'Connor, F. M., Roberts,
 544 M. J., Rodriguez, J. M., Woodward, S., Best, M. J., Brooks, M. E., Brown, A. R., Butchart,
 545 N., Dearden, C., Derbyshire, S. H., Dharssi, I., Doutriaux-Boucher, M., Edwards, J. M.,
 546 Falloon, P. D., Gedney, N., Gray, L. J., Hewitt, H. T., Hobson, M., Huddleston, M. R.,
 547 Hughes, J., Ineson, S., Ingram, W. J., James, P. M., Johns, T. C., Johnson, C. E., Jones, A.,
 548 Jones, C. P., Joshi, M. M., Keen, A. B., Liddicoat, S., Lock, A. P., Maidens, A. V., Manners,
 549 J. C., Milton, S. F., Rae, J. G. L., Ridley, J. K., Sellar, A., Senior, C. a., Totterdell, I. J.,
 550 Verhoef, A., Vidale, P. L. and Wiltshire, A.: The HadGEM2 family of Met Office Unified
 551 Model climate configurations, *Geosci. Model. Dev.*, 4, 723-757, doi:10.5194/gmd-4-723-
 552 2011, 2011.

553 Morgenstern, O., Braesicke, P., O'Connor, F. M., Bushell, C. A., Johnson, C. E., Osprey, S.
 554 M. and Pyle, J. A.: Model development evaluation of the new UKCA climate-composition
 555 model – Part 1 : The stratosphere, *Geosci. Model Dev.*, 2, 43-57, doi:10.5194/gmd-2-43-
 556 2009, 2009.

557 Murray, L. T., Mickley, L. J., Kaplan, J. O., Sofen, E. D., Pfeiffer, M. and Alexander, B.:
 558 Factors controlling variability in the oxidative capacity of the troposphere since the Last
 559 Glacial Maximum, *Atmos. Chem. Phys. Discuss.*, 13, 24517-24603, doi:10.5194/acpd-13-
 560 24517-2013, 2013.

561 O'Connor, F. M., Johnson, C. E., Morgenstern, O., Abraham, N. L., Braesicke, P., Dalvi, M.,
 562 Folberth, G. A., Sanderson, M. G., Telford, P. J., Voulgarakis, A., Young, P. J., Zeng, G.,
 563 Collins, W. J. and Pyle, J. A.: Evaluation of the new UKCA climate-composition model –
 564 Part 2: The troposphere, *Geosci. Model Dev.*, 7, 41-91, doi:10.5194/gmd-7-41-2014, 2014.

565 Ott, L. E., Pickering, K. E., Stenchikov, G. L., Allen, D. J., DeCaria, A. J., Ridley, B., Lin,
 566 R.-F., Lang, S. and Tao, W.-K.: Production of lightning NO_x and its vertical distribution
 567 calculated from three-dimensional cloud-scale chemical transport model simulations, *J.*
 568 *Geophys. Res.*, 115, D04301, doi:10.1029/2009JD011880, 2010.

569 Pickering, K. E., Wang, Y., Tao, W.-K., Price, C. and Müller, J.-F.: Vertical distributions of
 570 lightning NO_x for use in regional and global chemical transport models, *J. Geophys. Res.*,
 571 103, 31203-31216, 1998.

572 Prather, M. J., Ehhalt, D., Dentener, F., Derwent, R., Dlugokencky, E., Holland, E., Isaksen,
 573 I., Katima, J., Kirchoff, V., Matson, P., Midgley, P. and Wang, M.: Atmospheric chemistry
 574 and greenhouse gases, in: *Climate Change 2001: The Scientific Basis. Contribution of*
 575 *Working Group I to the Third Assessment Report of the Intergovernmental Panel on Climate*
 576 *Change*, Houghton, J. T., Ding, Y., Griggs, D. J., Noguer, M., van der Linden, P. J., Dai, X.,
 577 Maskell, K., and Johnson, C. A., Cambridge University Press, Cambridge, UK, 329–287,
 578 2001.

579 Price, C. and Rind, D.: A simple lightning parameterization for calculating global lightning
 580 distributions, *J. Geophys. Res.*, 97, 9919-9933, 1992.

581 Price, C. G. and Rind, D.: Modeling global lightning distributions in a general circulation
 582 model, *M. Weather Rev.*, 122, 1930-1939, 1994a.

583 Price, C. G. and Rind, D.: Possible implications of global climate change on global lightning
584 distributions and frequencies, *J. Geophys. Res.*, 99, 10823-10831, 1994b.

585 Price, C. G.: Lightning applications in weather and climate research, *Surv. Geophys.*, 34,
586 755-767, doi:10.1007/s10712-012-9218-7, 2013.

587 Rayner, N. A., Parker, D. E., Horton, E. B., Folland, C. K., Alexander, L. V., Rowell, D. P.,
588 Kent, E. C. and Kaplan, A.: Global analyses of sea surface temperature, sea ice, and night
589 marine air temperature since the late nineteenth century, *J. Geophys. Res.*, 108, 4407,
590 doi:10.1029/2002JD002670, 2003.

591 Russo, M. R., Marécal, V., Hoyle, C. R., Arteta, J., Chemel, C., Chipperfield, M. P., Dessens,
592 O., Feng, W., Hosking, J. S., Telford, P. J., Wild, O., Yang, X. and Pyle, J. A.:
593 Representation of tropical deep convection in atmospheric models – Part 1: Meteorology and
594 comparison with satellite observations, *Atmos. Chem. Phys.*, 11, 2765-2786,
595 doi:10.5194/acp-11-2765-2011, 2011.

596 Ryu, J.-H. and Jenkins, G. S.: Lightning-tropospheric ozone connections: EOF analysis of
597 TCO and lightning data, *Atmos. Environ.*, 39, 5799-5805,
598 doi:10.1016/j.atmosenv.2005.05.047, 2005.

599 Schumann, U. and Huntrieser, H.: The global lightning-induced nitrogen oxides source,
600 *Atmos. Chem. Phys.*, 7, 2623-2818, doi:10.5194/acpd-7-2623-2007, 2007.

601 Stevenson, D. S., Young, P. J., Naik, V., Lamarque, J.-F., Shindell, D. T., Voulgarakis, A.,
602 Skeie, R. B., Dalsoren, S. B., Myhre, G., Berntsen, T. K., Folberth, G. A., Rumbold, S. T.,
603 Collins, W. J., MacKenzie, I. A., Doherty, R. M., Zeng, G., van Noije, T. P. C., Strunk, A.,
604 Bergmann, D., Cameron-Smith, P., Plummer, D. A., Strode, S. A., Horowitz, L., Lee, Y. H.,
605 Szopa, S., Sudo, K., Nagashima, T., Josse, B., Cionni, I., Righi, M., Eyring, V., Conley, A.,
606 Bowman, K. W., Wild, O. and Archibald, A.: Tropospheric ozone changes, radiative forcing
607 and attribution to emissions in the Atmospheric Chemistry and Climate Model
608 Intercomparison Project (ACCMIP), *Atmos. Chem. Phys.*, 13, 3063-3085, doi:10.5194/acp-
609 13-3063-2013, 2013.

610 Thompson, A. M., Stewart, R. W., Owens, M. A. and Herwehe, J. A.: Sensitivity of
611 tropospheric oxidants to global chemical and climate change, *Atmos. Environ.*, 23, 519-532,
612 1989.

613 Telford, P. J., Abraham, N. L., Archibald, A. T., Braesicke, P., Dalvi, M., Morgenstern, O.,
614 O'Connor, F. M., Richards, N. A. D. and Pyle, J. A.: Implementation of the Fast-JX
615 Photolysis scheme (v6.4) into the UKCA component of the MetUM chemistry-climate model
616 (v7.3), *Geosci. Model. Dev.*, 6, 161-177, doi:10.5194/gmd-6-161-2013, 2013.

617 Thompson, A. M., Stewart, R. W., Owens, M. A. and Herwehe, J. A.: Sensitivity of
618 tropospheric oxidants to global chemical and climate change, *Atmos. Environ.*, 23, 519-532,
619 1989.

620 van Vuuren, D. P., Edmonds, J., Kainuma, M., Riahi, K., Thomson, A., Hibbard, K., Hurtt,
621 G. C., Kram, T., Krey, V., Lamarque, J.-F., Masui, T., Meinshausen, M., Nakicenovic, N.,
622 Smith, S. J. and Rose, S. K.: The representative concentration pathways: an overview, *Clim.*
623 *Change*, 109, 5-31, doi:10.1007/s10584-011-0148-z, 2011.

624 Voulgarakis, a., Naik, V., Lamarque, J.-F., Shindell, D. T., Young, P. J., Prather, M. J., Wild,
625 O., Field, R. D., Bergmann, D., Cameron-Smith, P., Cionni, I., Collins, W. J., Dalsøren, S.
626 B., Doherty, R. M., Eyring, V., Faluvegi, G., Folberth, G. a., Horowitz, L. W., Josse, B.,
627 MacKenzie, I. a., Nagashima, T., Plummer, D. a., Righi, M., Rumbold, S. T., Stevenson, D.
628 S., Strode, S. a., Sudo, K., Szopa, S. and Zeng, G.: Analysis of present day and future OH and
629 methane lifetime in the ACCMIP simulations, *Atmos. Chem. Phys.*, 13, 2563-2587,
630 doi:10.5194/acp-13-2563-2013, 2013.

631 Wild, O., Fiore, A. M., Shindell, D. T., Doherty, R. M., Collins, W. J., Dentener, F. J.,
632 Schultz, M. G., Gong, S., MacKenzie, I. A., Zeng, G., Hess, P., Duncan, B. N., Bergmann, D.
633 J., Szopa, S., Jonson, J. E., Keating, T. J. and Zuber, A.: Modelling future changes in surface
634 ozone: a parameterized approach, *Atmos. Chem. and Phys.*, 12, 2037-2054, doi:10.5194/acp-
635 12-2037-2012, 2012.

636 Williams, E. R.: Lightning and climate: a review, *Atmos. Res.*, 76, 272-287,
637 doi:10.1016/j.atmosres.2004.11.014, 2005.

638 WMO: Meteorology - a three-dimensional science: second session of the Commission for
639 Aerology, *WMO Bull.*, 4, 134-138, 1957.

640 Wong, J., Barth, M. C. and Noone, D.: Evaluating a lightning parameterization based on
641 cloud-top height for mesoscale numerical model simulations, *Geosci. Model. Dev.*, 6, 429-
642 443, doi:10.5194/gmd-6-429-2013, 2013.

643 Xie, S.-P., Deser, C., Vecchi, G. a., Ma, J., Teng, H. and Wittenberg, A. T.: Global warming
644 pattern formation: sea surface temperature and rainfall, *J. Clim.*, 23, 966-986,
645 doi:10.1175/2009JCLI3329.1, 2010.

646 Young, P. J., Archibald, A. T., Bowman, K. W., Lamarque, J.-F., Naik, V., Stevenson, D. S.,
647 Tilmes, S., Voulgarakis, A., Wild, O., Bergmann, D., Cameron-Smith, P., Cionni, I., Collins,
648 W. J., Dalsøren, S. B., Doherty, R. M., Eyring, V., Faluvegi, G., Horowitz, L. W., Josse, B.,
649 Lee, Y. H., MacKenzie, I. A., Nagashima, T., Plummer, D. A., Righi, M., Rumbold, S. T.,
650 Skeie, R. B., Shindell, D. T., Strode, S. A., Sudo, K., Szopa, S. and Zeng, G.: Pre-industrial
651 to end 21st century projections of tropospheric ozone from the Atmospheric Chemistry and
652 Climate Model Intercomparison Project (ACCMIP), *Atmos. Chem. Phys.*, 13, 2063-2090,
653 doi:10.5194/acp-13-2063-2013, 2013.

654 Zeng, G. and Pyle, J. A.: Changes in tropospheric ozone between 2000 and 2100 modeled in
655 a chemistry-climate model, *Geophys. Res. Lett.*, 30, 1-4, doi:10.1029/2002GL016708, 2003.

656 Zeng, G., Pyle, J. A. and Young, P. J.: Impact of climate change on tropospheric ozone and
657 its global budgets, *Atmos. Chem. Phys.*, 8, 369-387, doi:10.5194/acp-8-369-2008, 2008.

658 Table 1. List of model simulations. The final two columns are averages over the 10 year
659 simulation periods.

Scenario	Climate (SSTs, sea ice, GHGs ^a)	ODS: Cl _y , Br _y ^b	Anthropogenic ozone precursor emissions ^c	LNO _x / Tg(N) yr ⁻¹	Tropospheric ozone burden / Tg(O ₃)
Base	2000	2000	2000	6.04	326
ΔODS	2000	2100 (RCP4.5)	2000	5.98	344
ΔO3pre	2000	2000	2100 (RCP4.5)	5.98	292
Δ(ODS+O3pre)	2000	2100 (RCP4.5)	2100 (RCP4.5)	6.05	308
ΔCC4.5	2100 (RCP4.5)	2000	2000	8.08	356
Δ(CC4.5+ODS)	2100 (RCP4.5)	2100 (RCP4.5)	2000	7.97	374
Δ(CC4.5+O3pre)	2100 (RCP4.5)	2000	2100 (RCP4.5)	8.01	319
ΔCC8.5	2100 (RCP8.5)	2000	2000	10.7	369
Δ(CC8.5+ODS)	2100 (RCP8.5)	2100 (RCP4.5)	2000	10.6	393
Δ(CC8.5+O3pre)	2100 (RCP8.5)	2000	2100 (RCP4.5)	10.6	337
Base(fLNO _x)	2000	2000	2000	6.04 ^d	325
ΔCC8.5(fLNO _x)	2100 (RCP8.5)	2000	2000	6.04 ^d	307

660 ^aThese are the changes in GHGs imposed within the radiation scheme only.

661 ^b Relative to Base, runs containing ΔODS include total chlorine (Cl_y) and total bromine (Br_y) reductions of 60-
662 70% (1.6 ppb) and 40-50% (9.4 ppt), respectively.

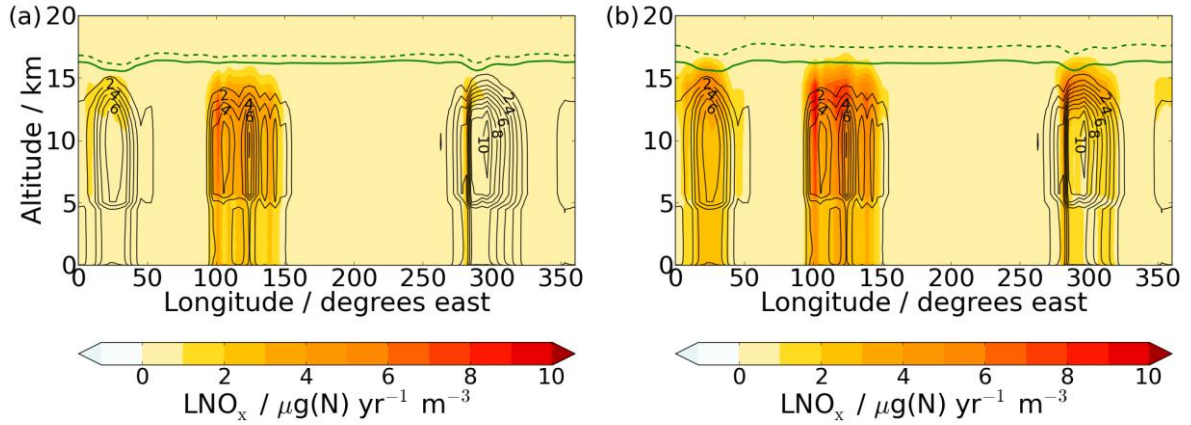
663 ^c Relative to Base, runs containing ΔO3pre include average global and annual emission changes of: NO(-51%),
664 CO (-51%), HCHO(-26%), C₂H₆ (-49%), C₃H₈ (-40%), H₃CCOCH₃ (-2%), CH₃CHO (-28%).

665 ^d LNO_x is not interactively calculated but imposed by applying a monthly mean climatology of the Base run.

666 Table 2. Tropospheric O_x budget of the Base run and changes from Base to ΔCC8.5 and
667 ΔCC8.5(fLNO_x).

	Base	ΔCC8.5-Base	ΔCC8.5(fLNO _x)-Base
Production / Tg(O ₃) yr ⁻¹	4870	980 (20.1%)	340 (7.0%)
Loss / Tg(O ₃) yr ⁻¹	4220	1090 (25.8%)	500 (11.8%)
Net chemical production / Tg(O ₃) yr ⁻¹	655	-109 (-16.6%)	-159 (-24.3%)
Deposition / Tg(O ₃) yr ⁻¹	1020	-10 (-1.0%)	-87 (-8.5%)
STE inferred* / Tg(O ₃) yr ⁻¹	360	101 (28.1%)	78 (21.7%)
Burden / Tg(O ₃)	326	43 (13.2%)	-19 (-5.8%)
Methane lifetime / yrs	7.60	-1.79 (-23.5%)	-1.04 (-13.8%)

668 * Stratosphere-troposphere exchange calculated as the residual from closure of the O_x budget.



669

670 Fig. 1. Annual mean, longitude-altitude cross sections of tropically averaged (20°S-20°N)
 671 LNO_x (contours) of the Base run and changes (shading) from Base to (a) ΔCC4.5 and (b)
 672 ΔCC8.5. Regions which show notable changes in LNO_x are: Central Africa (0-50°E), the
 673 Maritime Continent (100-150°E) and South America (280-320°E). Solid (Base run) or dashed
 674 (future runs) green lines indicate the height of the thermal tropopause, which is calculated
 675 based on the WMO lapse rate definition (WMO, 1957).

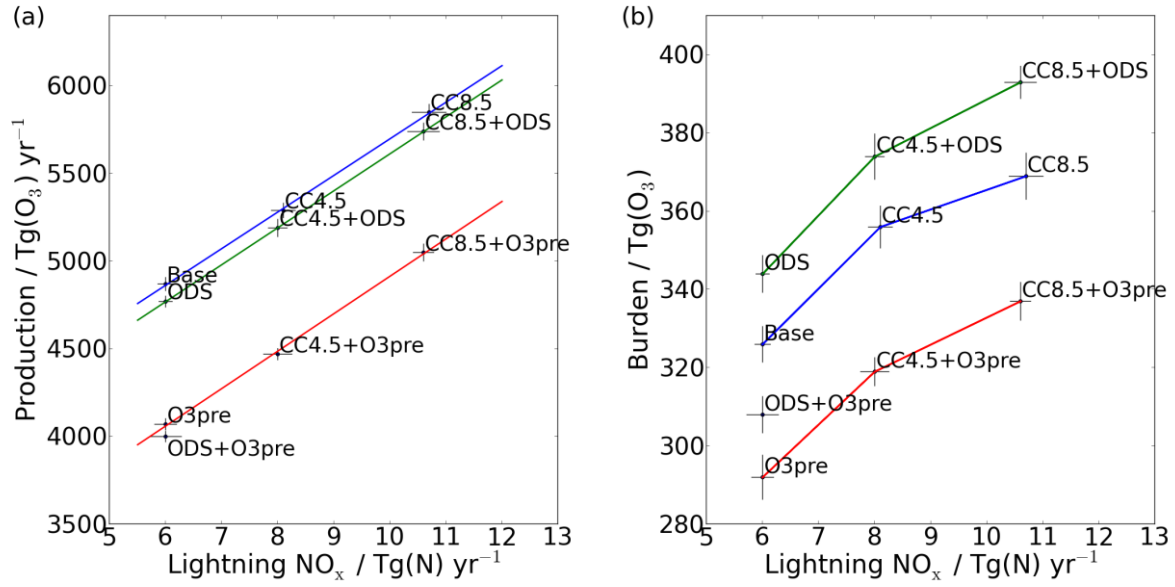
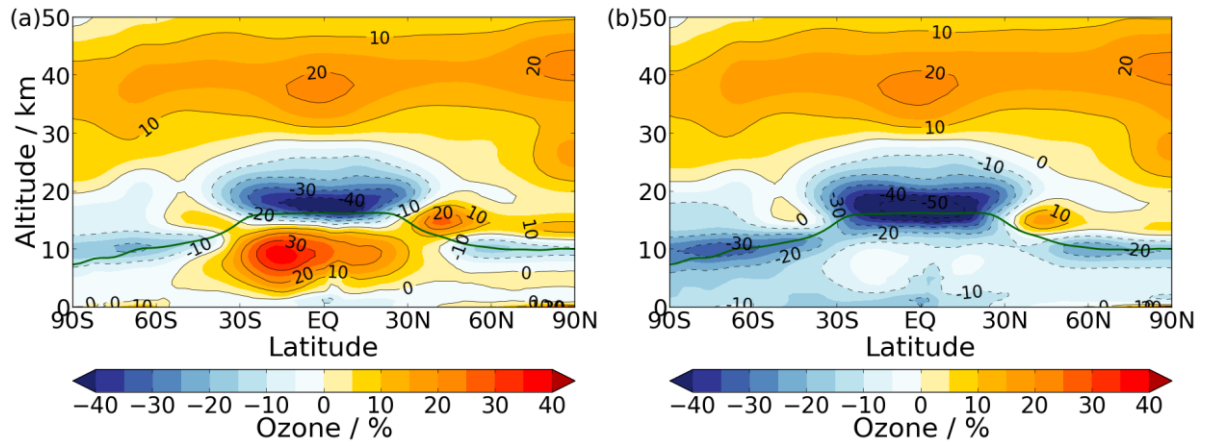


Fig. 2. Correlation between (a) $P(O_3)$ and LNO_x and (b) tropospheric ozone burden and LNO_x . Linear fits in (a) and connecting lines in (b) are drawn between runs which differ only in their climate states. Error bars indicate ± 1 standard deviation.



680

681 Fig. 3. Annual mean, zonal mean changes (shading and contours) in ozone (%) relative to
 682 Base for (a) $\Delta\text{CC8.5}$ and (b) $\Delta\text{CC8.5}(\text{fLNO}_x)$. Solid green lines indicate the height of the
 683 thermal tropopause of the Base run.

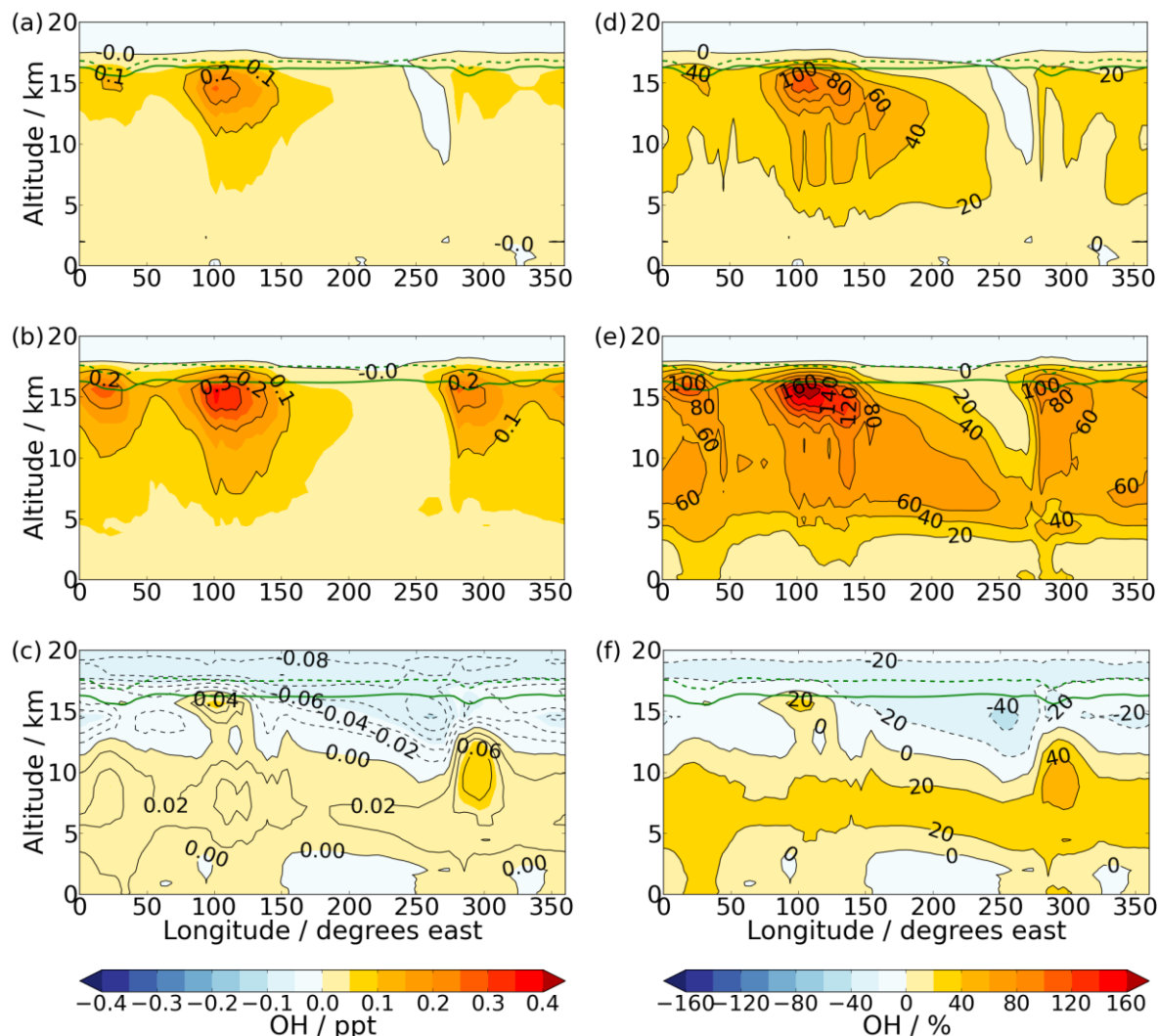


Fig. 4. Annual mean, longitude-altitude cross sections of tropically averaged (20°S - 20°N) changes (shading and contours) in OH mixing ratios (ppt) from Base to (a) $\Delta\text{CC4.5}$ (b) $\Delta\text{CC8.5}$ and (c) $\Delta\text{CC8.5(fLNO}_x\text{)}$; the differences as a percentage of the Base values for (d) $\Delta\text{CC4.5}$ (e) $\Delta\text{CC8.5}$ and (f) $\Delta\text{CC8.5(fLNO}_x\text{)}$. Solid (Base run) or dashed (future runs) green lines indicate the height of the thermal tropopause.